Nuclear Instruments and Methods in Physics Research A 631 (2011) 6–11

Contents lists available at ScienceDirect

Nuclear Instruments and Methods in Physics Research A

journal homepage: www.elsevier.com/locate/nima

Micro-collimators fabricated by chemical etching of thin polyallyldiglycol carbonate polymer films exposed to oxygen ions

V.W.Y. Choi [a], C.K.M. Ng [a], D. Nikezic [a], T. Konishi [b], K.N. Yu [a,*]

[a] Department of Physics and Materials Science, City University of Hong Kong, Tat Chee Avenue, Kowloon Tong, Hong Kong
[b] National Institute of Radiological Sciences, Department of Technical Support & Development, Chiba 263-8555, Japan

ARTICLE INFO

Article history:
Received 30 August 2010
Received in revised form
6 December 2010
Accepted 12 December 2010
Available online 21 December 2010

Keywords:
Solid-state nuclear track detector
SSNTD
α Particle
PADC
Collimator

ABSTRACT

One approach for α particle radiobiological experiments is to use solid-state nuclear track detectors (SSNTDs) as support substrates to record the α particle hit positions on the targets. To facilitate accurate characterization of the hit positions as well as the incident α particle energies, micro-collimators are required in these experiments to restrict the incident α particles to those with small deviations from normal incidence with respect to the collimator. In the present paper, we fabricated micro-collimators, which restricted α particles to those with deviations as low as 12°. Specially etched polyallyldiglycol carbonate (PADC) films, which are a kind of SSNTD, with a thickness 70 μm were prepared from commercially available PADC films. These were then irradiated by 4.83 MeV/n oxygen ions generated from the heavy-ion medical accelerator in Chiba (HIMAC), Japan. The irradiated films were chemically etched for at least 2.7 h to achieve etched-through air channels to form the micro-collimators. The micro-collimators formed by etching the irradiated films for 2.7, 3.0 and 4.0 h were experimentally shown to be able to restrict α particles to those very close to normal incidence. In contrast, the micro-collimator formed by etching the irradiated film for 4.5 h started to allow α particles with larger deviations from normal incidence to pass through, which is likely due to overlapping of air channels from excessive etching.

1. Introduction

Studies on biological effects of α particles are important because (1) α particle irradiation is ubiquitous in our natural environment, which arise from our inhalation of radon progeny [1–5] and (2) α particles have large linear energy transfer (LET) values and are efficient in causing DNA double strand breaks (DSBs) [6–9]. In α particle radiobiological experiments where the targets (such as cultured cells or other organisms) are irradiated with α particles, it is necessary to determine the dose absorbed by the targets, which requires the accurate positions and incident energies of α particle hits on the targets.

There are different approaches to determine the number and energy of α particles actually incident on the targets. The first one is to make use of versatile microbeam facilities in which the hit positions and the energies of the incident ions can be precisely controlled but will involve sophisticated equipment and instrumentation [10–15]. Columbia's group also developed a stand-alone microbeam without a conventional accelerator as a source of energetic ions, but focused α particles from an α emitter using a compound magnetic lens consisting of 24 permanent magnets arranged in two quadrupole triplets [16].

Another approach is to make use of a radioactive α particle source such as ^{241}Am without focusing. However, due to the statistical nature of radioactivity and the random direction of α particle emission, both the hit positions and the energies of the α particles cannot be controlled. For this method, researchers have made use of solid-state nuclear track detectors (SSNTDs) as support substrates of the targets, which can record the hit positions of α particles and reveal these on subsequent chemical etching, to help determine the hit positions retrospectively (see Refs. [17–28]). A review on SSNTDs was given by Nikezic and Yu [29]. The targets are irradiated with α particles, which pass through the SSNTD substrate to strike the targets in contact with the substrate. However, the incident angle of the α particles on the substrate will vary due to the random direction of α particle emission. Excessively oblique incidence will make accurate determination of hit positions difficult and at the same time will necessitate tedious procedures to determine the resultant energy of the α particles incident onto the target. To tackle this problem, Choi et al. [30] recently proposed the use of a micro-collimator to screen out those α particles insufficiently close to normal incidence with respect to the surface of the support substrate. The micro-collimator was an etched polyallyldiglycol carbonate (PADC) film, which was an SSNTD and commercially sometimes available as the CR-39

* Corresponding author. Tel.: +852 3442 7812; fax: +852 3442 0538.
E-mail address: peter.yu@cityu.edu.hk (K.N. Yu).

0168-9002/$ - see front matter © 2010 Elsevier B.V. All rights reserved.
doi:10.1016/j.nima.2010.12.100

detector. PADC films have become popular support substrates for cell culture with track registration capability in that they are transparent, biocompatible [31] and are not dissolved in the alcohol used for sterilizing the substrate.

The micro-collimator fabricated by Choi et al. [30] was 15 μm thick; so the energy loss of α particles while traveling through the air columns in the collimator was minimized. By approximating an air channel as a frustum of a cone, the semi-cone angle was found to be ~23°. As commented by Choi et al. [30], it is desirable to fabricate mirco-collimators with more cylindrical bores, i.e., those with smaller semi-cone angles, so that the α particles passing through the collimators will be closer to normal incidence. With the help of surfactants (5% DOWFAX 2A1) in the etchant, Choi et al. [30] succeeded to fabricate mirco-collimators with semi-cone angles of ~20°. In the present paper, we proposed an alternative method to fabricate micro-collimators to restrict passing α particles to those even closer to normal incidence with respect to the substrate surface by making use of the high-energy heavy ions generated from the heavy-ion medical accelerator in Chiba (HIMAC). The fabricated micro-collimators were characterized and the results were discussed.

2. Methodology

2.1. Preparation of PADC films

In the present work, PADC films with thicknesses of both 1 mm and 100 μm commercially available from Page Mouldings (Pershore) Limited, Worcestershire, were employed.

Here we first describe our use of the 100 μm PADC films. For different purposes, thin PADC films with different thicknesses smaller than 100 μm were prepared using the method proposed by Chan et al. [22]. Briefly, they were chemically etched in a 1 N NaOH/ethanol solution at 40 °C, for which the bulk etch rate was about 10 μm h^{-1} [32]. During the chemical etching in NaOH/ethanol, sodium carbonate was accumulated on the surface of the PADC films, which would reduce the etching rate [32]. As such, the films were rinsed with distilled water every 2 h to maintain an efficient etching. Thin PADC films with thickness less than 100 μm had also been fabricated by other groups [20,33–35] but the methodology or the applications were different.

In the present work, two films with size of 1.8 cm × 1.8 cm were cut from a 100 μm PADC film and were etched to predetermined thicknesses. The incident oxygen ions had an energy of 4.83 MeV/n when they reached the sample (see Section 2.2 below). According to the SRIM program (http://www.srim.org/), these oxygen ions were in a range of 73.3 μm in the PADC films. The first etched film was used to determine the relationship between the track length and the etching time, which was needed to determine the total etching time to achieve etched-through air channels in a PADC film. As such, this film was etched to a thickness of 74 μm, and the total etching time required to achieve etched-through air channels in this film will be slightly larger than the etching time required to achieve etched-through air channels in all films with oxygen ions actually passing through them (i.e., in all films with thickness smaller than 73.3 μm). The second etched film was used for the actual fabrication of micro-collimators with the help of the relationship determined from etching the first film. For this purpose, we chose the final thickness of the etched PADC film to be 70 μm, which was smaller than the range of the oxygen ions. Apart from these two films, thin PADC films with 20 μm thickness were also prepared as support substrates to be used in Section 2.5 as a part of the setup to characterize the micro-collimators fabricated in Section 2.4.

On the other hand, the thicker 1 mm PADC films were directly employed, i.e., without etching or other preparation, as α recorders to be used in Section 2.5 also as a part of the setup to test the micro-collimators fabricated in Section 2.4.

2.2. Oxygen-ion irradiation of the thin PADC films

The PADC films with thicknesses of 74 and 70 μm fabricated as described in Section 2.1 were irradiated by oxygen ions generated from the heavy-ion medical accelerator in Chiba (HIMAC). HIMAC is a heavy-ion synchrotron for medical use and began its operation in November 1993 [36]. In addition to medical use, research activities, e.g., in the field of physics and biology, were also conducted using the HIMAC facilities [37]. The HIMAC irradiation system has been previously reviewed by Konishi et al. [38]. With regard to the oxygen ions, they were accelerated to 6.0 MeV/n by the linear accelerator. These 6 MeV/n ions were introduced into the Medium Energy Beam Experiments (MEXP) beam course after bending the beam by a 90° magnet. The oxygen ions went through three 1 μm thick Al foils (secondary electron monitor or SEM) and a 6 μm Havar foil (beam exit window) installed in the beam line, and were then extracted into a 21 mm air gap between the Havar foil and the sample. The energy of the oxygen ions would become 4.83 MeV/n when the ions reached the sample, according to calculations using SRIM. The distance between the irradiation point and the exit window could be chosen. The oxygen-ion fluence could be determined by using PADC SSNTDs [38]. The fluence measured in this study was 3×10^3 particles/mm^2.

2.3. Relationship between track length and etching time

The 74 μm PADC film was used to study the relationship between the track length and the etching time. After oxygen-ion irradiation, the 1.8 cm × 1.8 cm film was cut into 5 pieces of rectangular films with a length of 1.8 cm and a width of ~0.36 cm. These 5 rectangular films were etched separately in 6.25 N NaOH/water at 70 °C for different etching periods, such as, 0.5, 1.0, 1.5, 2.0 and 2.5 h. During this double-sided chemical etching, the latent tracks left by the oxygen ions were fixed, with the track depth increased and the track opening (i.e., the major and minor axes, or the diameter of the tracks) enlarged (see e.g., Ref. [29]).

The track lengths were determined from the cross-sectional images of the tracks. For this purpose, an etched PADC film needed to be first embedded in a resin. Before pouring the resin into the mold, which is a cylindrical plastic cup with a detachable bottom, the inside surface of the mold was coated with a releasing agent (Buehler, USA). The etched PADC film was then placed onto the bottom of the mold. A blended fluid was prepared by thoroughly mixing 10 parts of Ultrathin 2 Epoxy Resin (Pace technologies, USA) with 1 part of Ultrathin 2 hardener (Pace technologies, USA) by weight, and was immediately poured into the mold with the PADC film inside. The resin was allowed to set for 1 day. The detachable bottom of the mold was then removed and the resin embedding the PADC film was released.

The resin embedding the etched PADC film was cut into two halves, perpendicularly to both the film surface and the longest side of the film, with the help of a saw (Lotusbrand), and one of the two exposed planar surfaces was polished using a water polisher. When the surface was polished, tracks were revealed. However, the true length of a track could only be given from the cross-section containing the tip of the etched track, by which time the measured length should also be maximum. As such, the length of the track should be monitored under an optical microscope (Nikon) throughout the polishing process. Images of the etched tracks were captured by a camera (Diagnostic Instruments Inc., Model: 25.4 2Mp Slider) attached to the microscope (Nikon) with a 1000 × magnification for further analyses.

2.4. Fabrication of the micro-collimators

The 70 μm PADC film was used for the actual fabrication of the micro-collimators with the help of the relationship determined from Section 2.3. After oxygen-ion irradiation, the 1.8 cm × 1.8 cm PADC film was cut into 9 pieces of 0.6 cm × 0.6 cm films. Five pieces were then mounted by epoxy (Araldite® Rapid, England) onto separate plastic sheets with a 0.4 cm × 0.4 cm rectangular opening at the center, and were then etched on both sides in 6.25 N NaOH/water at 70 °C for etching periods of 1.0, 2.7, 3.0, 4.0 and 4.5 h. During this chemical etching, the latent tracks left by the oxygen ions were fixed, with the track depth increased and the track opening enlarged. Images of the track openings on these micro-collimators were captured by a camera attached to the microscope with 200 × magnification.

2.5. Testing the micro-collimators

To test the properties of the micro-collimators, we made use of the experimental setup previously devised by Choi et al. [30]. The micro-collimator was inserted between the α particle source and the support substrate so that only those α particles close to normal incidence onto the micro-collimator could pass through. On top of the support substrate was another PADC film, which was used to record the α particles after they had passed through the support substrate, and we referred this PADC film as the α recorder. In real irradiation experiments, these α particles would strike the cultured cells or other targeted organisms instead of the α recorder.

As described in Section 2.1, in the present experiments, thick PADC films with 1 mm thickness were employed as α recorders, while thin PADC films with 20 μm thickness were used as support substrates. The number and incident angles of α particles passing through the micro-collimators were assessed by examining the α particle tracks generated on the corresponding α recorders. A planar ^{241}Am source with an activity of 0.115 μCi was employed for α particle irradiation, and the irradiation time was 4 min. The α recorders were then etched in 6.25 N NaOH/water at 70 °C for 3.0 h to enlarge the tracks on the samples. Images of the enlarged tracks were captured from a camera attached on a microscope with magnification 200 ×. The optical appearance of the tracks were examined.

3. Results and discussion

3.1. Relationship between track length and etching period

As described in Section 2.3, five pieces of rectangular films with a length of 1.8 cm, a width of ~0.36 cm and a thickness of 74 μm PADC film, which were irradiated with 4.83 MeV/n oxygen ions, were used to study the relationship between the track length and the etching time. These films were etched separately in 6.25 N NaOH/water at 70 °C for different etching periods, such as, 0.5, 1.0, 1.5, 2.0 and 2.5 h, and were then embedded in resin. The resin embedding an etched PADC film was cut into two halves, perpendicular to both the film surface and the longest side of the film, and one of the two planar surfaces was polished using a water polisher.

Since the oxygen ions passed through the PADC film and double-sided chemical etching was involved, tracks would develop along the latent tracks from both film surfaces. An example showing the cross-sectional images of the tracks is given in Fig. 1. Here, the film had been etched in 6.25 N NaOH/water at 70 °C for 2.0 h, and was observed to be sandwiched between two layers of resin. In Fig. 1, the region outlined by the dotted line shows two conical tracks formed along the same ion trajectory in opposite directions. At this stage, these two opposite tracks had not touched and etched-through air channel had not yet been achieved.

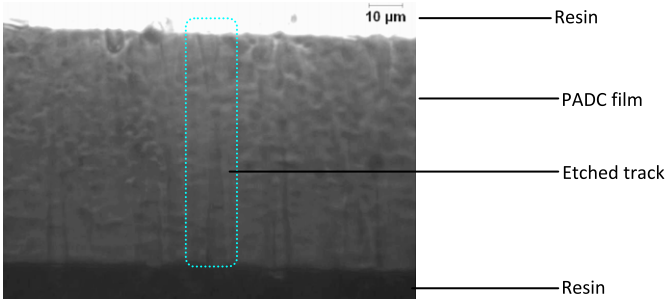

Fig. 1. Cross-sectional image of a PADC film with tracks generated by 4.83 MeV/n oxygen ions and etched in 6.25 N NaOH/water at 70 °C for 2.0 h. The film is sandwiched between two layers of resin. The dotted region shows two conical tracks formed along the same ion trajectory in opposite directions.

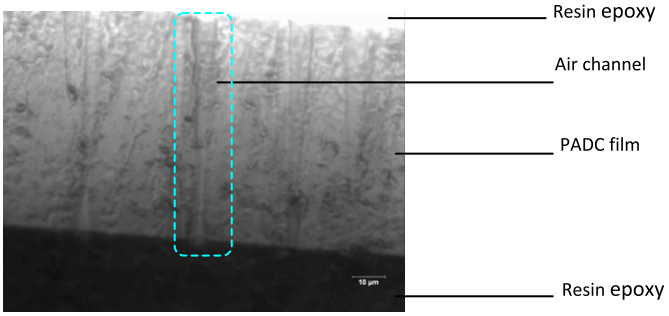

Fig. 2. Cross-sectional image of a PADC film with etched-through air channels generated by 4.83 MeV/n oxygen ions and etched in 6.25 N NaOH/water at 70 °C for 2.5 h. The film is sandwiched between two layers of resin. The dotted region shows an air channel formed by joining two conical tracks formed along the same ion trajectory in opposite directions.

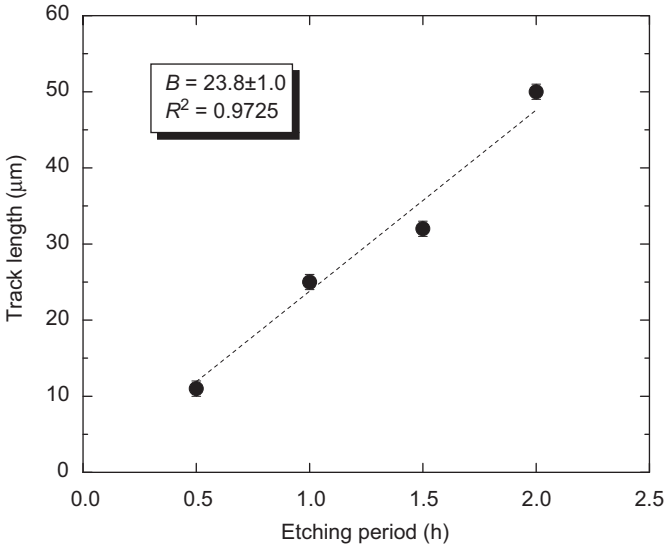

Fig. 3. Relationship between the measured track length and the etching period. Solid line: best fit line $y = Bx$, with the best fit parameter B and the corresponding 95% confidence interval shown in the inset.

From such cross-sectional images, the lengths of the longer tracks were determined using the computer software ImageJ freely obtained from the website http://rsb.info.nih.gov/ij/. The longer tracks, which corresponded to larger LET values, were developed from the film surface from where the oxygen ions exit the film. Etched-through air channels were achieved after 2.5 h of etching. An

example showing the cross-sectional images of these air channels is given in Fig. 2. Here, the film had been etched in 6.25 N NaOH/water at 70 °C for 2.5 h. The region outlined by the dotted line in Fig. 2 shows an air channel formed by joining two conical tracks formed along the same ion trajectory in opposite directions.

The overall results are shown in Fig. 3 and summarized in Table 1. It can also be observed from Fig. 3 that the track length increases almost linearly with the etching period, with an increase rate of $\sim$25 μm h^{-1}. The single-side bulk etch rate was also determined from the residual thickness of the etched PADC films as 1.08 μm h^{-1}, which was very close to our previous values of 1.10 ± 0.02 and 1.20 ± 0.03 μm h^{-1} obtained for etching under magnetic stirring and under no stirring, respectively, and for the same brand of PADC films [39]. Adding the bulk etch rate of $\sim$1 μm h^{-1} to the track length increase rate of $\sim$25 μm h^{-1}, the track etch rate is $\sim$26 μm h^{-1}. For comparison, the track etch rate for oxygen ions with an energy of 26.41 MeV is $\sim$20 μm h^{-1} in TASTRAK (Track Analysing Systems Ltd., UK) PADC films etched in 7.25 N NaOH/water at 70 °C (with a bulk etch rate of 1.73 ± 0.05 μm h^{-1}) [40].

Table 1
Track length as a function of etching period. Residual thicknesses of the etched PADC films measured using ImageJ are also shown.

Etching period (h)	Track length (μm)	Residual thickness of etched PADC film (μm)
0.5	11	72.8
1.0	25	71.7
1.5	32	70.8
2.0	50	69.6
2.5	Etched through	68.6

3.2. Fabricating and testing the micro-collimators

As described in Section 2.4, nine pieces of 0.6 cm × 0.6 cm films with a thickness of 70 μm, which were irradiated with 4.83 MeV/n oxygen ions, were used to fabricate the micro-collimators. Five pieces were separately mounted by epoxy onto five plastic sheets with a 0.4 cm × 0.4 cm rectangular opening at the center, and were then etched on both sides in 6.25 N NaOH/water at 70 °C for etching periods of 1.0, 2.7, 3.0, 4.0 and 4.5 h. From Section 3.1, etched-through air channels were achieved after 2.5 h of etching. However, these were achieved for a PADC film with a thickness of 74 μm; so the etching time required to achieve etched-through air channels here for a 70 μm film is expected to be less than 2.5 h. Nevertheless, taking into account different uncertainties, we used 2.7 h as the minimum etching time for the fabrication of the micro-collimators.

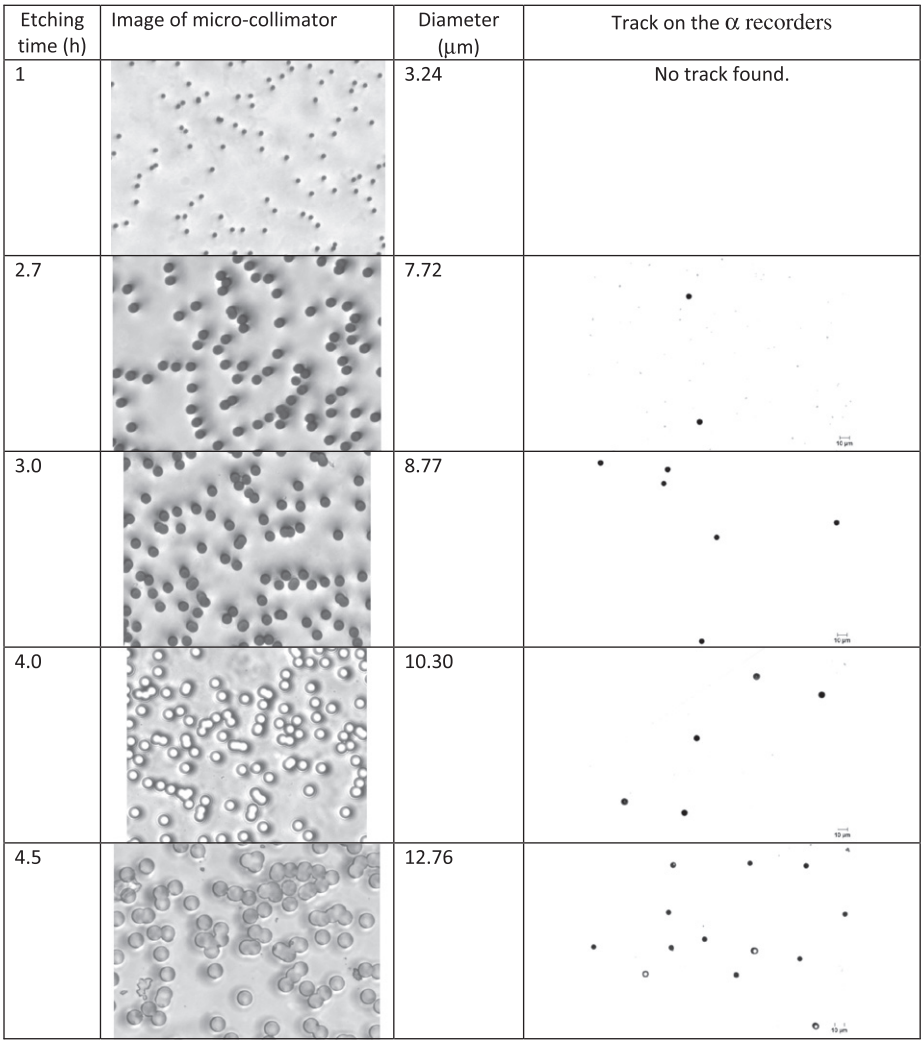

Fig. 4. Images of irradiated PADC films etched for different periods, and the α particle tracks on the corresponding α recorders, both captured by a camera attached to the microscope with 200 × magnification. Column 1: etching periods; column 2: images of the PADC films etched for different periods; column 3: pore diameters determined from images in column 2; column 4: images of α particle tracks on the corresponding α recorders.

Fig. 4 shows the images of micro-collimators prepared by etching the 70 μm PADC films irradiated with oxygen ions and etched on both sides for 2.7, 3.0, 4.0 and 4.5 h. The images were captured by a camera attached to the microscope with 200 × magnification. The final thickness and the pore diameter on these micro-collimators were 63 and 7.72 μm for 2.7 h etching, 63 and 8.77 μm for 3.0 h etching and 58 and 10.3 μm for 4.0 h etching.

At the same time, the image of another 70 μm PADC film also irradiated by oxygen ions but etched on both sides for only 1.0 h was also shown for comparison. As etched-through air channels were not expected to form with only 1 h etching time, this would not form a micro-collimator.

To test the properties of the micro-collimators, we made use of the experimental setup previously devised by Choi et al. [30]. The thick PADC films with 1 mm thickness employed as α recorders were irradiated with 5.49 MeV α particles from a planar ^{241}Am source with an activity of 0.115 μCi for 4 min through the corresponding micro-collimator as well as a 20 μm support substrate. The α recorders were then etched in 6.25 N NaOH/water at 70 °C for 3.0 h, and the images captured from a camera attached on a microscope with magnification 200 × are shown in Fig. 4. The α particles could indeed pass through the collimators (i.e., irradiated 70 μm PADC films further etched for 2.7, 3.0, 4.0 and 4.5 h) and formed tracks on the α recorders. This provides another solid evidence of the presence of etched-through air channels in these collimators. Moreover, for the micro-collimators formed by etching the irradiated films for 2.7, 3.0, 4.0 h, all the tracks on the α recorders were circular in shape meaning that the α particles passing through these micro-collimators hit the targets close to normal incidence. In contrast, for the micro-collimator formed by etching the irradiated films for 4.5 h, some tracks started to deviate from the circular shape, meaning that this micro-collimator started to allow α particles with larger deviations from normal incidence to pass through. A likely reason for the tracks deviating from the circular shape is the overlapping of air channels due to excessive etching. On the other hand, for a PADC film etched for only 1.0 h, no tracks were formed on the α recorder, showing that etched-through air channels were not achieved.

3.3. Measuring and simulating performance of micro-collimators

The energy spectra of α particles from an ^{241}Am source after passing through the fabricated micro-collimators (70 μm PADC films irradiated with oxygen ions and etched on both sides for 2.7, 3.0 and 4.0 h) were collected using an ORTEC SOLOIST α spectrometer (model number: 4001 A), and are shown in Fig. 5. The α spectrometer could only give spectra with α particle energies beyond 3.5 MeV. From Fig. 5, we can see very sharp energy peaks at the emitted α particle energy of 5.49 MeV. Furthermore, there are small background signals at α particle energies lower than the peak energy, particularly for the micro-collimator etched for 4.0 h. Monte Carlo simulations of the energy spectra are also given in Fig. 5 for a comparison, with normalization to the experimental data at 3.6 MeV. The small background signals at α particle energies lower than the peak energy are also reproduced by the simulations. Detailed analyses of the events causing these background signals revealed that they were generated when the α particles had slightly oblique paths partially in air in a bore of the micro-collimator and partially in the PADC material surrounding the bore.

Fortunately, the relative significance of these small background signals will be reduced after the α particles exiting from the micro-collimators further pass through a PADC film substrate, which is needed in radiobiological experiments. Fig. 6 shows the energy distributions of α particles emerging through a PADC film substrate with different thicknesses on top of a micro-collimator fabricated by irradiating a 70 μm PADC film with oxygen ions and then etched on both sides for 4.0 h. From Fig. 6, we can see that the energy peaks are very sharp and the small background signals at α particle energies lower than the peak energies are negligible.

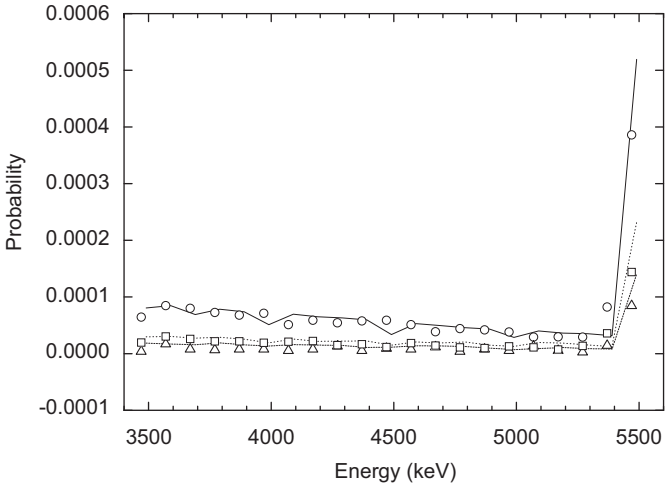

Fig. 5. Energy spectra of α particles from an ^{241}Am source after passing through the fabricated micro-collimators (70 μm PADC films irradiated with oxygen ions and etched on both sides for 2.7, 3.0 and 4.0 h). Outlined symbols: experimental data collected using an α spectrometer; outlined triangles: etched for 2.7 h; outlined squares: etched for 3.0 h and outlined circles: etched for 4.0 h. Lines: results from Monte Carlo simulations; dashed line: etched for 2.7 h; dotted line: etched for 3.0 h and solid line: etched for 4.0 h.

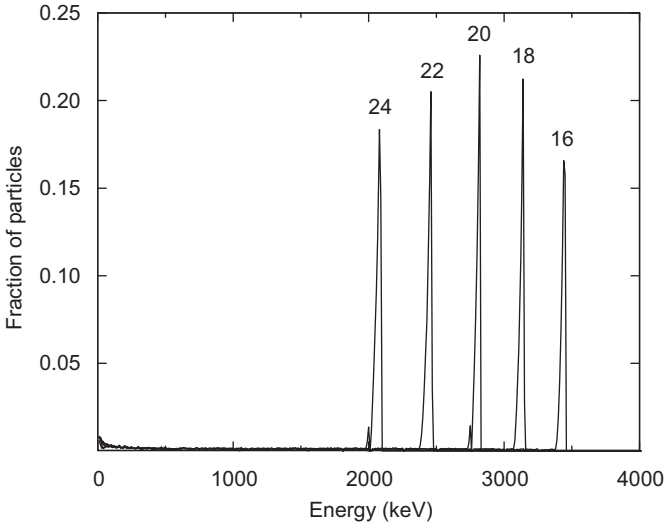

Fig. 6. Energy distribution of α particles emerging through a PADC film substrate with the shown thickness (in μm). The α particles have an initial energy of 5.49 MeV (from an ^{241}Am source) and pass through a micro-collimator with a thickness of 58 μm and a pore diameter of 10.3 μm (fabricated by irradiating a 70 μm PADC film with oxygen ions and then etched on both sides for 4.0 h) before hitting the PADC film substrate.

The angular distribution of α particles emerging through the PADC film substrate will also critically determine the performance of a micro-collimator. Fig. 7 shows the angular distributions of α particles (with respect to the normal to the surface of the substrate) emerging through a PADC film substrate with different thicknesses on top of a micro-collimator fabricated by irradiating a 70 μm PADC film with oxygen ions and then etched on both sides for 4.0 h. From Fig. 7, we can see that the angular distribution becomes increasingly narrower when the thickness of the PADC film substrate increases. When the substrate is 24 μm thick, all α particles

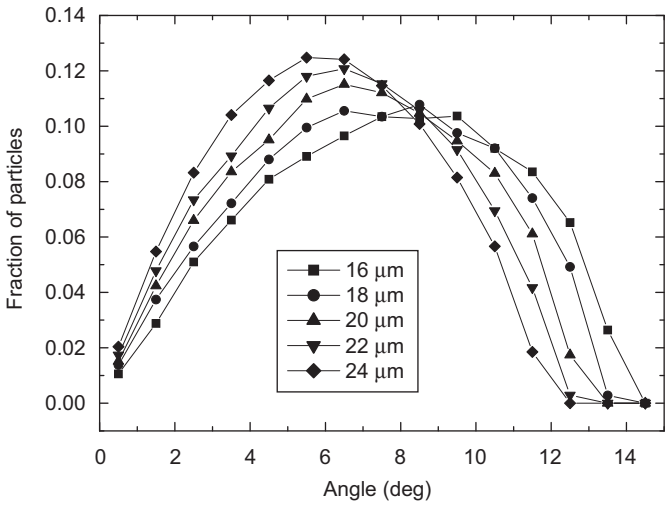

Fig. 7. Angular distribution of α particles (with respect to the normal to the surface of the substrate) emerging through a PADC film substrate with the shown thickness. The α particles have an initial energy of 5.49 MeV (from an ^{241}Am source) and pass through a micro-collimator with a thickness of 58 μm and a pore diameter of 10.3 μm (fabricated by irradiating a 70 μm PADC film with oxygen ions and then etched on both sides for 4.0 h) before hitting the PADC film substrate.

emerging through the substrate will have incidence angles (with respect to the normal to the surface of the substrate) smaller than 12° (smaller than 10° for more than 90% of the particles), which is sufficiently small to facilitate accurate characterization of the hit positions.

4. Conclusions

In the present paper, we proposed a method to fabricate micro-collimators to restrict α particles to those with deviations from normal incidence with respect to the collimator surface. Commercially available PADC films with a thickness of 100 μm were first etched to a thickness of 70 μm, which were then irradiated by 4.83 MeV/n oxygen ions. These were chemically etched for at least 2.7 h to achieve etched-through air channels to form the micro-collimators. An experimental setup was employed to test the characteristics of these micro-collimators through the study of the α particle tracks formed on a PADC film (referred to as the α recorder) by α particles from an ^{241}Am source that actually passed through the micro-collimators. It was found that α particles could indeed pass through the micro-collimators, which provided a solid evidence of the presence of etched-through air channels in these collimators. Moreover, for the micro-collimators formed by etching the irradiated films for 2.7, 3.0 and 4.0 h, all the tracks on the α recorders were circular in shape meaning that the α particles passing through these micro-collimators hit the targets close to normal incidence. Computer simulations confirmed that α particles having passed through a micro-collimator (the one etched for 4 h used as an example) and then a PADC film substrate (with thicknesses from 16 to 24 μm) became almost mono-energetic and had very narrow angular distributions (with respect to the normal to the surface of the substrate). The dominance of α particles close to normal incidence would facilitate more convenient and accurate dosimetric determinations in α particle radiobiological experiments.

Acknowledgments

This study was supported by the research project with heavy ions (19-B413) at NIRS-HIMAC. We would like to thank Ms. Mayu Isono from Metropolitan University Tokyo for helping set up the beam line and with irradiation in HIMAC-MEXP and Ms. Kumiko Kodama for assistance with ion fluence analysis.

References

[1] K.N. Yu, T.F. Chan, E.C.M. Young, Health Phys. 68 (1995) 716.
[2] K.N. Yu, E.C.M. Young, K.C. Li, Radiat. Prot. Dosim. 63 (1996) 55.
[3] K.N. Yu, E.C.M. Young, M.J. Stokes, Z.J. Guan, K.W. Cho, Health Phys. 73 (1997) 373.
[4] K.N. Yu, T. Cheung, Z.J. Guan, E.C.M. Young, B.W.N. Mui, Y.Y. Wong, J. Environ. Radioact. 45 (1999) 291.
[5] K.N. Yu, B.M.F. Lau, D. Nikezic, J. Hazard. Mater. 132 (2006) 98.
[6] W. Friedland, M. Dingfelder, P. Jacob, H.G. Paretzke, Radiat. Phys. Chem. 72 (2005) 279.
[7] K.M. Prise, M. Pinto, H.C. Newman, B.D. Michael, Radiat. Res. 156 (2001) 572.
[8] H.C. Newman, K.M. Prise, M. Folkard, B.D. Michael, Int. J. Radiat. Biol. 71 (1997) 347.
[9] D.J. Brenner, J.F. Ward, Int. J. Radiat. Biol. 61 (1992) 737.
[10] K.M. Prise, G. Schettino, B. Vojnovic, O. Belyakov, C. Shao, J. Radiat. Res. 50 (Suppl. A) (2009) A1.
[11] T.K. Hei, L.K. Ballas, D.J. Brenner, C.R. Geard, J. Radiat. Res. 50 (Suppl. A) (2009) A7.
[12] S. Gerardi, J. Radiat. Res. 50 (Suppl. A) (2009) A13.
[13] Y. Kobayashi, T. Funayama, N. Hamada, T. Sakashita, T. Konishi, H. Imaseki, K. Yasuda, M. Hatashita, K. Takagi, S. Hatori, K. Suzuki, M. Yamauchi, S. Yamashita, M. Tomita, M. Maeda, K. Kobayashi, N. Usami, L. Wu, J. Radiat. Res. 50 (Suppl. A) (2009) A29.
[14] M. Durante, J. Radiat. Res. 50 (Suppl. A) (2009) A55.
[15] H. Matsumoto, M. Tomita, K. Otsuka, M. Hatashita, J. Radiat. Res. 50 (Suppl. A) (2009) A67.
[16] G. Garty, G.J. Ross, A.W. Bigelow, G. Randers-Pehrson, D.J. Brenner, Radiat. Prot. Dosim. 122 (2006) 292.
[17] M. Durante, G.F. Grossi, M. Pugliese, L. Manti, M. Nappo, G. Gialanella, Nucl. Instr. and Meth. B 94 (1994) 251.
[18] B. Dörschel, D. Hermsdorf, S. Pieck, S. Starke, H. Thiele, F. Weickert, Nucl. Instr. and Meth. B 207 (2003) 154.
[19] S. Gaillard, C.J. Ross, V. Armbruster, M.A. Hill, D.L. Stevens, T. Gharbi, M. Fromm, Radiat Meas. 40 (2005) 279.
[20] S. Gaillard, V. Armbruster, M.A. Hill, T. Gharbi, M. Fromm, Radiat. Res. 163 (2005) 343.
[21] T. Konishi, K. Amemiya, T. Natsume, A. Takeyasu, N. Yasuda, Y. Furusawa, K. Hieda, J. Radiat. Res. 48 (2007) 255.
[22] K.F. Chan, B.M.F. Lau, D. Nikezic, A.K.W. Tse, W.F. Fong, K.N. Yu, Nucl. Instr. and Meth. B 263 (2007) 290.
[23] K.F. Chan, E.H.W. Yum, C.K. Wan, W.F. Fong, K.N. Yu, Nucl. Instr. and Meth. B 262 (2007) 128.
[24] K.F. Chan, E.H.W. Yum, C.K. Wan, W.F. Fong, K.N. Yu, Radiat. Meas. 43 (Suppl. 1) (2008) S541.
[25] Y.L. Law, K.N. Yu, Radiat. Meas. 44 (2009) 1069.
[26] T.P.W. Wong, A.K.W. Tse, W.F. Fong, K.N. Yu, Radiat. Meas. 44 (2009) 1081.
[27] E.H.W. Yum, C.K.M. Ng, A.C.C. Lin, S.H. Cheng, K.N. Yu, Nucl. Instr. and Meth. B 264 (2007) 171.
[28] E.H.W. Yum, V.W.Y. Choi, D. Nikezic, V.W.T. Li, S.H. Cheng, K.N. Yu, Radiat. Meas. 44 (2009) 1077.
[29] D. Nikezic, K.N. Yu, Mater. Sci. Eng. R 46 (2004) 51.
[30] V.W.Y. Choi, E.H.W. Yum, K.N. Yu, Nucl. Instr. and Meth. A 619 (2010) 211–215.
[31] W.Y. Li, K.F. Chan, A.K.W. Tse, W.F. Fong, K.N. Yu, Nucl. Instr. and Meth. B 248 (2006) 319.
[32] K.C.C. Tse, D. Nikezic, K.N. Yu, Nucl. Instr. and Meth. B 263 (2007) 300.
[33] T. Yamauchi, S. Watanabe, A. Seto, K. Oda, N. Yasuda, R. Barillon, Radiat. Meas. 43 (2008) S106.
[34] T. Yamauchi, Y. Mori, K. Oda, N. Yasuda, H. Kitamura, R. Barillon., Jpn. J. Appl. Phys. 47 (2008) 3606.
[35] Y. Mori, T. Ikeda, T. Yamauchi, A. Sakamoto, H. Chikada, Y. Honda, K. Oda, Radiat. Meas. 44 (2009) 211.
[36] H. Tsujii, J. Mizoe, T. Kamada, M. Baba, H. Tsuji, H. Kato, S. Kato, S. Yamada, S. Yasuda, T. Ohno, T. Yanagi, R. Imai, K. Kagei, H. Kato, R. Hara, A. Hasegawa, M. Nakajima, N. Sugane, N. Tamaki, R. Takagi, S. Kandatsu, K. Yoshikawa, R. Kishimoto, T. Miyamoto, J. Radiat. Res. 48 (2007) A1.
[37] T. Murakami, H. Tsujii, Y. Furusawa, K. Ando, T. Kanai, S. Yamada, K. Kawachi, J. Nucl. Mater. 248 (1997) 360.
[38] T. Konishi, N. Yasuda, A. Takeyasu, S. Ishizawa, T. Fujisaki, K. Matsumoto, Y. Furusawa, Y. Sato, K. Hieda, Rev. Sci. Instr. 76 (2005) 114302.
[39] J.P.Y. Ho, C.W.Y. Yip, D. Nikezic, K.N. Yu, Radiat. Meas. 36 (2003) 141.
[40] B. Dörschel, D. Hermsdorf, S. Starke, Radiat. Meas. 37 (2003) 583.